Nucl Eng Technol 47 (2015) 662–668

Available online at www.sciencedirect.com

ScienceDirect

journal homepage: http://www.journals.elsevier.com/nuclear-engineering-and-technology/

Original Article

INTERPARTICLE POTENTIAL OF 10 NANOMETER TITANIUM NANOPARTICLES IN LIQUID SODIUM: THEORETICAL APPROACH

SOO JAE KIM [a], GUNYEOP PARK [a], HYUN SUN PARK [b,*], MOO HWAN KIM [c], and JEHYUN BAEK [a]

[a] Department of Mechanical Engineering, POSTECH, 77 Cheongam-Ro, Nam-Gu, Pohang, Gyungbuk 37673, Republic of Korea
[b] Division of Advanced Nuclear Engineering, POSTECH, 77 Cheongam-Ro, Nam-Gu, Pohang, Gyungbuk 37673, Republic of Korea
[c] Korea Institute of Nuclear Safety, 62 Gwahak-Ro, Yuseong-Gu, Daejeon 34142, Republic of Korea

ARTICLE INFO

Article history:
Received 28 March 2015
Received in revised form
27 May 2015
Accepted 2 June 2015
Available online 11 August 2015

Keywords:
Ab initio calculation
Liquid sodium
Sodium–water reaction
Solvation potential
Titanium Nanoparticle
Van der Waals forces

ABSTRACT

A suspension of titanium nanoparticles (Ti NPs) in liquid sodium (Na) has been proposed as a method to mitigate the violent sodium–water reaction (SWR). The interparticle potential between Ti NPs in liquid Na may play a significant role in the agglomeration of NPs on the reaction surface and in the bulk liquid Na, since the potential contributes to a reduction in the long-term dispersion stability. For the effective control of the SWR with NPs, a physical understanding of the molecular dynamics of NPs in liquid Na is key. Therefore in this study, the nonretarded Van der Waals model and the solvation potential model are employed to analyze the interparticle potential. The *ab initio* calculation reveals that a strong repulsive force driven by the solvation potential exceeds the interparticle attraction and predicts the agglomeration energy required for two 10-nm Ti NPs to be 4×10^{-17} J. The collision theory suggests that Ti NPs can be effective suppressors of the SWR due to the high energy barrier that prevents significant agglomeration of Ti NPs in quiescent liquid Na.

1. Introduction

Sodium (Na) is an excellent coolant as it has extremely high thermal conductivity, low neutron flux, low meting temperature, and high boiling temperature. Therefore, in the development of the next-generation nuclear reactor design, Na-coolant-based reactors have become one of the key design concepts in the GEN-IV program [1]. However, it is well known that when Na comes into direct contact with water or moist air, a sodium–water reaction (SWR) occurs. This violent exothermic reaction rapidly releases a large amount of heat, gases including explosive H_2, and corrosive NaOH. In 1995, a

* *Corresponding author.*
E-mail address: hejsunny@postech.ac.kr (H.S. Park).

http://dx.doi.org/10.1016/j.net.2015.06.007
1738-5733/Copyright © 2015, Published by Elsevier Korea LLC on behalf of Korean Nuclear Society.

Na leakage accident occurred at the Monju reactor in Japan. In the accident, Na leaked from a pipe and reacted with water causing a fire intense enough to warp steel structures. The lesson learned from the accident was that the elimination of SWR risk should be one of the most significant design criteria for the development of safe sodium fast cooled reactors.

When a leakage occurs in the Na and water heat exchanger, the pressurized water in the secondary loop intrudes into liquid Na, causing an energetic SWR. Therefore, development of technologies to prevent or mitigate SWR becomes a key issue in the fast cooled reactor design. One method involves isolating Na from water by employing a double-walled piping system and guard vessels [1–4]. This technology, however, cannot be an ultimate solution, since the probability of failure of the system still exists. An alternative method is to reduce or eliminate SWR. In this area, recent studies [5–11] suggested that a small quantity of nanoparticles (NPs) suspended in Na reduced the reaction rate between Na and water. The studies showed that the hydrogen production rate and reaction heat generation during the SWR were reduced when titanium (Ti) NPs with 2 at% and 0.214 vol % for 10 nm and <100 nm, respectively, were mixed in the liquid Na. However, it is necessary to further understand the mechanism.

The strong attraction between Na atoms and Ti NP surfaces reduces SWR reactivity [6,7,11], increases liquid Na surface tension by 16%, and reduces its evaporation rate by 18% [6]. Dispersed NPs constrain the movement of many nearby Na atoms, which therefore cannot easily react with H_2O. The SWR can only occur where NPs are not present; this observation indicates that the NPs reduce the effective area of the reaction surface [12], and that areal density of NPs (NPs/m^2) at the Na/H_2O interface is a key parameter that affects the effectiveness of NPs to suppress reactivity.

If NPs are well dispersed and evenly hold Na atoms, as illustrated in Fig. 1A, the reactivity would be reduced effectively. However, when NPs agglomerate into clusters over time, the effective area of the reaction surface increases, thus lowering the effectiveness of NPs to reduce SWR reactivity (Fig. 1B). For this reason, the effectiveness of NPs in mitigating SWR can be determined by the agglomeration behavior of NPs at the Na/H_2O interface over time. Unfortunately, experimental observation of NPs in bulk liquid Na and the reaction surface is difficult, since SWR is very fast and liquid Na is visually opaque. Therefore, in this study, the agglomeration behavior of NPs was analytically studied and theoretically discussed by employing the non-retarded Van der Waals and solvation potential models to evaluate the interparticle potential between 10-nm Ti NPs in liquid Na. In this paper, the computational methodology for the theoretical analysis is described in the second section, the analytical result from the computation is discussed in the third section, and the final conclusion of the study will follow.

2. Materials and methods

2.1. *Computation method*

In order to understand the behavior of colloidal particles in a liquid medium, the force between the particles should be known. Many types of forces act on NPs in liquids; a force can be categorized by its origins as a Van der Waals, an electrostatic, a solvation, an entropic, or a nonequilibrium force [13]. Van der Waals, a relatively weak force, always exists, and it can be attractive or repulsive with respect to the interparticle distance. An electrostatic force, a relatively strong force, arises when a particle is polarized. Coulomb, hydrogen bonding, and electric double-layer forces are typical examples of electrostatic forces. If the charged particles are in a vacuum, Coulomb force will act; however, in nature, this is a rare case. In most cases, neutral colloidal particles are in a specific solvent such as water. Particles in a solvent are polarized due to the ions that are absorbed from the solvent; the electric double-layer force arises due to the oppositely charged ions surrounding the particles. The electric double-layer force is a repulsive force and its strength is proportional to the ion concentration. In the past, most studies have used Van der Waals and electric double-layer forces in order to depict colloidal particle dispersion and stability; this approach is named the Derjaguin and Landau, Verwey and Overbeek (DLVO) theory [14,15]. The DLVO theory predicts the behavior of colloidal particles in typical electrolytes reasonably well when the particles are separated by tenths of a nanometer. However, when the particle distance is lower than a Debye

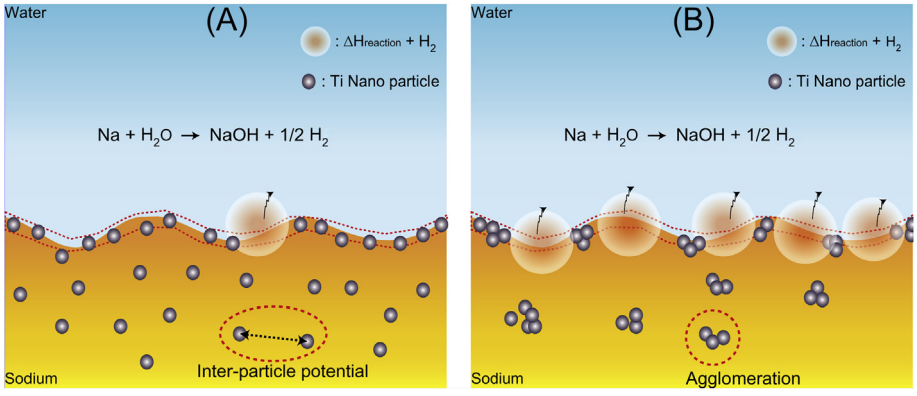

Fig. 1 – Effect of suspended Ti nanoparticles on the sodium–water reaction. (A) Well-dispersed state and (B) agglomerated state.

length [16] (generally a few nm) or the structure of the system is complex such as biomolecules, the DLVO theory often fails [13,17] due to the assumptions made in the theory that are not valid anymore. The DLVO theory assumes solvent ions or atoms as points and ignores the specific structure of particle surfaces. However, this is not valid when the particles are larger than the solvent atom size. In order to correct the DLVO theory, non-DLVO-type forces have been studied [17]; solvation and entropic forces are typical examples of non-DLVO forces. If solvent atoms interact with the surface of colloidal particles, the number density of the solvent atoms will be different from that of the solvent atoms in a bulk state; this variation in solvent atom number density results in the solvation force. The solvation force becomes a dominant force when there is a strong interaction between solvent atoms and colloidal particle surfaces [18–22]. Strictly speaking, a smooth surface cannot exist, and the roughness of colloidal particle surfaces leads to the entropic force. The entropic force becomes important in biomolecules, which have a thermally mobile interface or surface.

In this study, the system consists of Ti NPs and liquid Na. In liquid Na, metallic bonded Na atoms share their electrons and the electron density tends to be uniform. If Na ions are created, electron density is perturbed locally and energy of the state is raised; therefore, stability and ion strength of Na ions in liquid Na are assumed to be very low. Ti atoms hold neighbor Ti atoms very strongly, so Ti NP surface is assumed to be smooth and thermally immobile. Based on these assumptions, the electric double-layer and entropic forces between Ti NPs were ignored. Since Na atoms and Ti NP surfaces have a strong chemical bonded interaction [12], the solvation force should be considered in our case. A nonequilibrium force, such as viscous and hydrodynamic force, is generated by dynamic movement of groups of molecules or particles. However, quantifying this force is not easy, so a quiescent flow condition assumption is made for ignoring this force. Therefore, in this study, the Van der Waals and solvation forces are considered.

2.1.1. *Nonretarded Van der Waals potential*

Since the Van der Waals interaction occurs when electrons are instantaneously perturbed, the strength of the interaction depends on the electron permeability of the medium and decreases (or is "retarded") with distance. Retardation of the Van der Waals potential can be neglected [13] if the distance is within a nanometer scale. The nonretarded Van der Waals potential energy [23] can be evaluated as follows:

$$U_{vdw}(D)[J] = -\frac{A_{121}}{6}\left\{\frac{2R^2}{(4R+D)D} + \frac{2R^2}{(2R+D)^2} + \ln\frac{(4R+D)D}{(2R+D)^2}\right\}. \quad (1)$$

In Eq. (1), the Hamaker constant, A_{121}, of Ti submerged in liquid Na can be assumed to be the combination of the Hamaker constants of each material in a vacuum [24] and evaluated using the Liftz theory [25]:

$$A_{121} \approx \left(\sqrt{A_1} - \sqrt{A_2}\right)^2,\ A_i = \frac{3}{4}kT + \frac{3}{16\sqrt{2}}h\upsilon_{e,i}. \quad (2)$$

Plasma frequencies of free electrons, ν_e, for each material are summarized in Table 1.

Table 1 – Plasma frequency of free electron for Na and Ti.

Material	ν_e (THz)	A (10^{-19} J)
Na	8,640 [26]	7.62
Ti	4,000 [27]	3.39

2.1.2. *Solvation potential*

In order to know the solvation potential between spherical particles, the formula for the solvation potential between semi-infinite flat surfaces [18] and Derjaguin's approximation [28] is applied. The solvation potential between semi-infinite flat surfaces is given as follows:

$$U_{Solv,flat}(D) = \int_D^\infty F_{Solv,flat}(\varsigma)d\varsigma = \int_D^\infty -\text{Area}\left\{\int_0^\varsigma \frac{\partial U_{lattice,2}(z)}{\partial z}\rho_2(z)dz - \int_0^\infty \frac{\partial U_{lattice,2}(z)}{\partial z}\rho_2(z)dz\right\}d\varsigma \quad (3)$$

where $U_{lattice,2}$ is the interatomic potential energy between the surface, and Na atoms and ρ_2 is the areal-averaged Na atom number density that changes with respect to the perpendicular distance z. If the flat surfaces are identical, the same force will act on Na atoms from each side; ρ_2 will be symmetric with respect to $z = D/2$. Using this assumption, ρ_2 can be assumed to be a function of the areal-averaged Na atom number density on one side of the surface, $\rho_{2,one\text{-}side}$ [18]:

$$\rho_2(z) \approx \frac{\rho_{2,one\text{-}side}(z)\rho_{2,one\text{-}side}(D-z)}{\rho_{2,bulk}} \quad (4)$$

$$\rho_{2,one\text{-}side}(z) \approx \rho_{2,bulk}\exp\left\{\frac{U_{lattice,2}(\infty) - U_{lattice,2}(z)}{k_BT} + \frac{4/3\pi\sigma^3\omega}{k_BT}\left(\rho_{2,bulk}(z) - \rho_{2,one\text{-}side}\right)\right\} \quad (5)$$

If an Na atom is in a chemical equilibrium, ρ_2 is proportional to the chemical potential. The chemical potential with respect to z consists of the potential energy and entropy. If the change of entropy is smaller than the change of potential energy, the change of chemical potential can be a function of the potential energy difference. The potential energy results from the interatomic forces between the surface and Na atoms, and between neighboring Na atoms. The potential energy difference of the Na–Na interaction was modeled as a function of ρ_2 and the cohesive energy ω of the bulk solid Na. Na atoms attract neighboring Na atoms when $\rho_{2,one\text{-}side}$ is lower than $\rho_{2,bulk}$, and repel them otherwise. Physically, if z is sufficiently large, $\rho_{2,one\text{-}side}$ should be the same as $\rho_{2,bulk}$; Eq. (5) satisfies this limitation. In Eq. (5), $U_{lattice,2}$ should be known to evaluate $\rho_{2,one\text{-}side}$. Steele [29] modeled the interatomic potential given to a gaseous molecule from the lattice surface as a combination of the electron Coulomb repulsive force and attractive force due to dispersion. This is a modified version of the Lennard–Jones potential model [30] commonly used for describing inert gases. However, it is not an adequate model for a system in which quantum mechanical effects have an important influence, since it cannot exactly describe the electron structure change. When an Na atom approaches an NP surface, their electron structures change and chemical

adsorption occurs [12], indicating that a more realistic model for $U_{lattice,2}$ is needed.

For modeling of $U_{lattice,2}$, the *ab initio* calculation (details are shown in [12]) is carried out using the density functional theory (Fig. 2). A five-layer structure with 60 hexagonally arranged Ti atoms is modeled to describe a flat crystalline surface. In the model, the two bottom layers are fixed to model the bulk Ti state, and the remaining layers are relaxed to model the Ti (0001) surface. Thermodynamically, the (0001) surface is the most stable face and depicted for modeling the Ti NP surface in this study. The perpendicular distance between Na atoms, z, is varied, and the electron structure changes with this distance. In order to evaluate the electron structure and total system energy, the Kohn–Sham equation [31,32] is solved using the quantum espresso [33]. The calculations are continued until the residual force on each relaxed Ti atom is below 1 meV/Å; to reduce the error caused by the periodic boundary condition, the distance between the periodic images along the z direction is set to be > 36 Å. The Brillouin zone integration to calculate electron density is performed with the Monkhorst–Pack mesh [34] with $(5 \times 5 \times 1)$ *k* points. The Methfessel–Paxton smearing method [34] is used for modeling electron occupation in the vicinity of the Fermi level.

The *ab initio* calculation result gives a similar trend to the Steele model [29] at $z > 1.5\sigma$ and has the minimum energy at 0.77σ (Fig. 2). In the case of $z < 1.5\sigma$, the Steele model predicts a larger increase than the *ab initio* calculation. This discrepancy between the *ab initio* calculation and the Steele model originates from the fact that the *ab initio* calculation considers the "exchange correlation." The "exchange correlation" is purely a quantum mechanical property that lowers the total system energy.

The solvation potential energy between semi-infinite flat plates can be mapped onto spherical particles separated by distance *D*. Derjaguin's approximation [28] that has been used for a finite body can be applicable to nanoscale bodies [35–38], as shown in Eq. (6):

$$U_{solv,\ spherical}(D) = 2\pi R \int_{D}^{\infty} \frac{U_{solve,\ flat}(\varsigma)}{\text{Area}} d\varsigma\,, \tag{6}$$

From Eqs. (3)–(6), the solvation potential energy among the 10-nm spherical Ti NPs separated by distance *D* was iteratively calculated.

3. Results

3.1. Areal-averaged Na atom number density distribution

Areal-averaged Na atom number density ρ_2 with respect to z is evaluated using Eqs. (4) and (5). In order to know the ρ_2 profile for various interparticle separation distances *D*, the normalized areal-averaged Na atom number density ρ_2/ρ_{bulk} is plotted with respect to z/*D* (Fig. 3). *D* is varied by multiples of the Na atom size, σ; z/*D* is varied from 0 to 1, which represents z from one side of the surface to the other side; and ρ_2/ρ_{bulk} is varied from 0 to 1.5 and is symmetric with respect to $z/D = 0.5$. When $D = 1\sigma$, only one Na atom can be at $z/D = 0.5$ and ρ_2 is the same as ρ_{bulk}. At this position, due to the symmetric approximation, Na atoms feel the same amount of force from every side of the surface but in opposite directions. Therefore, Na has no interaction with the surface, and Na atoms are stacked as bulk liquid Na because it is energetically favorable. When $D = 2\sigma$, ρ_2/ρ_{bulk} has its maximum as 1.48 at $z/D = 0.5$; this indicates

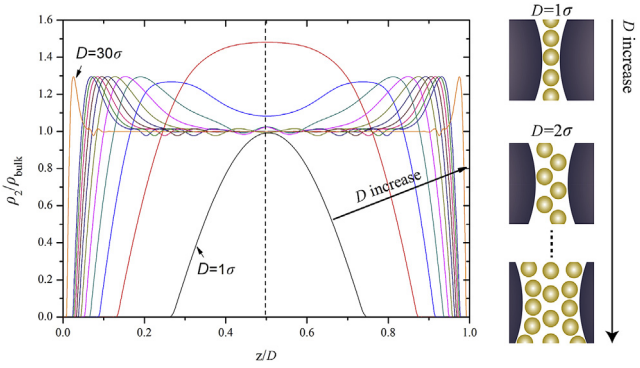

Fig. 3 – Normalized sodium atom number density with respect to *D*.

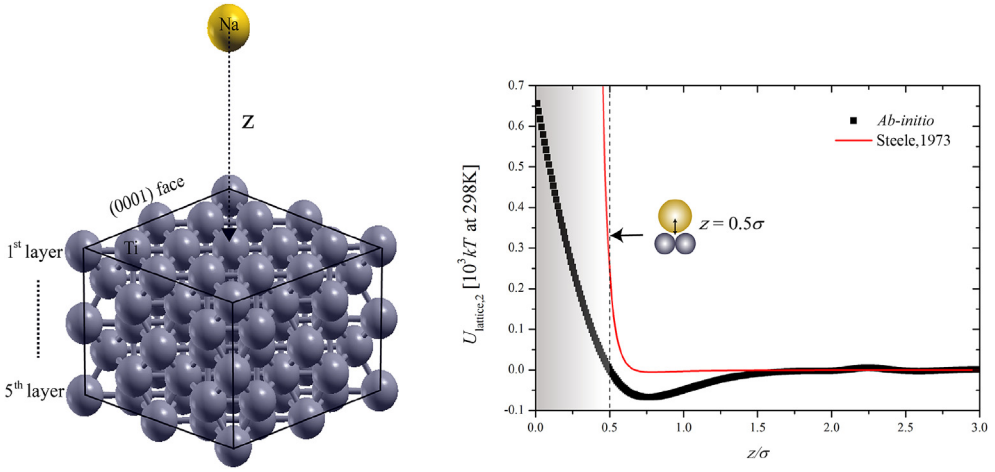

Fig. 2 – Modeling of *ab initio* calculation and results.

that Na atoms are stacked as a staggered configuration. Like the case of $D = 1\sigma$, at $z/D = 0.5$, Na atoms have no forces from the surface and only feel their neighboring Na atoms. However, differently from the $D = 1\sigma$ case, ρ_2 is 1.48 times higher than ρ_{bulk}; this indicates that $D = 2\sigma$ is a confined and energetically unfavorable geometry. Based on ρ_2/ρ_{bulk} at $z/D = 0.5$ for various D values, this energetically unfavorable situation continues until $D = 7\sigma$. When $D > 7\sigma$, ρ_2/ρ_{bulk} has its maximum in the vicinity of each particle surface due to the interatomic interaction between Na atoms and the surface.

In short, Fig. 3 shows that when $2\sigma < D < 7\sigma$, the geometry is too confined and energetically unfavorable, so Ti NPs in liquid Na are more energetically favorable to have $D > 7\sigma$ without considering Van der Waals interaction between NPs.

3.2. *Interparticle potential and force*

In order to discuss NP agglomeration and dispersion stability, the Van der Waals, salvation, and total potential energies of the system are plotted with respect to the normalized interparticle separation distance D/σ, as shown in Fig. 4. D/σ varies from 0 to 7, which is about 0–3 nm; illustrations that explain the situation at $D = 0.04\sigma$ and 7σ have been added. From $D = 7\sigma$ to $D = 0$, the Van der Waals potential energy decreases from 0 to −2,543 kT, while the solvation potential energy increases from 0 to 10,871 kT. Magnitudes of both potential energies increase as D decreases; the total system potential energy increases from $D = 0$ to $D = 0.04\sigma$ and decreases at $0.04\sigma < D < 7\sigma$. This indicates that the solvation potential is dominant at $D > 0.04\sigma$; this matches reasonably well with the conclusion from the section on areal-averaged Na atom number density distribution, with the confined Na atoms being energetically unfavorable at $D < 7\sigma$. The total force acting on each Ti NP is evaluated with respect to D/σ from the derivative of the total potential energy (Fig. 5). Repulsive force acts on the NP at $D > 0.03\sigma$ and the maximum repulsive force is 3.6×10^{-7} N at $D = 0.12\sigma$. An attractive force acts on the NP at $D < 0.03\sigma$; no force acts on the NP at $D \geq 7\sigma$. From the results, if two Ti NPs approach within $D = 0.03\sigma$, which is about 0.1 Å, they attract each other and will finally be agglomerated; the energy

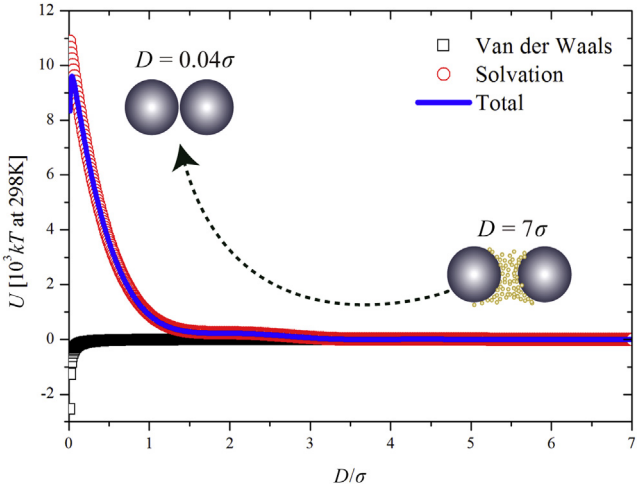

Fig. 4 – Interparticle potential between 10-nm Ti nanoparticles.

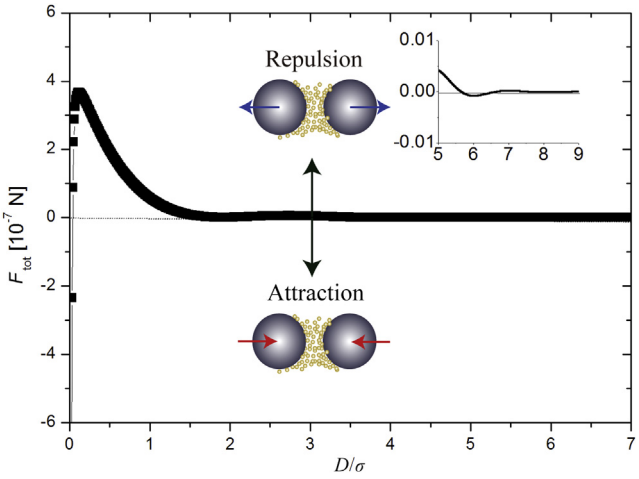

Fig. 5 – Total force between 10-nm Ti nanoparticles.

required for agglomeration of two NPs is approximately 9,630 kT at 298 K (~4×10^{-17} J). The total potential energy and the force have been evaluated, but the physical meaning of this amount of energy is still ambiguous.

In order to get physical insights from the results, the probability of agglomeration of NPs at a specific temperature and NP content are evaluated with some assumptions. Assuming that NP agglomeration follows the collision theory [39], the probability of agglomeration, P_{col}, is inversely proportional to the energy barrier ΔE_a, which is 9,630 kT in this study:

$$P_{col} = \frac{1}{(\tau_{agg}/\tau_{col})} \approx e^{-\frac{\Delta E_a}{kT}} \quad (7)$$

where the NP collision time τ_{col} can be defined as follows:

$$\tau_{col} \approx \frac{D_{mean}}{v_{Np}} \approx \left(\frac{M_{Np}}{N_A \rho_{Na} \phi}\right)^{1/3} \left(\sqrt{\frac{3kT}{m_{Np}}}\right)^{-1}. \quad (8)$$

If NPs are initially well dispersed and cubically stacked, the mean distance between NPs, D_{mean}, will be inversely proportional to the weight fraction Φ of the NPs, as shown in Eq. (8). When the flow effect is negligible and the system is in thermal equilibrium at T K, the average kinetic energy of NPs will be $3kT/2$, where the number 3 represents the degrees of freedom of particles in this study. Therefore, the average velocity of the NPs, V_{Np}, will be proportional to the system temperature. From Eqs. (7) and (8), the time needed to form an agglomerate, τ_{agg}, of the 10-nm Ti NPs can be calculated based on the system temperature and NP content. Due to the extremely low $P_{col} \sim e^{-2,495}$, τ_{total} becomes infinite, although the system temperature reaches 1150 K, which is the boiling point of liquid Na, regardless of the NP content. This indicates that the agglomeration process cannot occur when the NPs are immersed into liquid Na due to the high repulsion force between them.

4. Discussion

Using the Van der Waals and solvation potential models, the interparticle potential among the 10-nm Ti NPs was analyzed to investigate the potential applicability of Ti-based NPs for SWR mitigation. Using the equation derived by Hamaker and

Liftz, the nonretarded Van der Waals potential was evaluated; the *ab initio* calculation based on the density functional theory was used to analyze the solvation potential. The analysis shows that the attractive interaction between Na atoms and the NP surface produces a strong repulsive solvation force, and a minimum energy of 4×10^{-17} J is required to agglomerate two NPs. Theoretically, this energy barrier and the collision theory [39] suggests that the 10-nm Ti NPs can be suspended in liquid Na without agglomeration, regardless of time, temperature, and NP content in quiescent flow conditions. Therefore, it is expected that the 10-nm Ti NPs can effectively suppress SWR over a sufficient time scale. However, these conclusions should be validated with experimental data, since a smooth Ti NP surface and quiescent flow condition do not exist in reality; roughness of the Ti NP surface can add the entropic force and liquid Na flow can add nonequilibrium forces, which have been ignored in this study.

Conflicts of interest

All contributing authors declare no conflicts of interest.

Acknowledgments

This work was supported by the National Research Foundation of Korea (NRF) grant funded by the Korean government (MSIP) (No. 2010–0018679) and the Supercomputing Center/Korea Institute of Science and Technology Information with supercomputing resources including technical support (KSC-2013-C3-066).

Nomenclature

A	Hamaker constant (J)
Area	NP surface area (m^2)
D	Shortest interparticle separation distance (m)
F	Force (N)
h	Plank constant (J second)
k	Boltzmann constant 1.38×10^{-23} (J/K)
kT	Energy unit ~4.11×10^{-21} ($T = 298$ K) (J)
M	Ti atomic weight (kg/mol)
m	NP mass (kg)
N_A	Avogadro's number (1/mol)
R	NP diameter (m)
V	Velocity (m/s)
U	Potential energy (J)

Greek letters

τ	NP collision time (seconds)
ω	Na–Na bond energy (J)
ρ	Number density and density of Na ($1/m^3$, kg/m^3)
σ	Atomic diameter of Na (m)
ν	Plasma frequency of free electrons (Hz)
Φ	NP weight fraction

Subscripts

1	Na
2	Ti
121	Na–Ti
bulk	Bulk liquid Na
e	Electron
i	Material index
Np	NP

REFERENCES

[1] K. Aoto, N. Uto, Y. Sakamoto, T. Ito, M. Toda, S. Kotake, Design study and R&D progress on Japan sodium-cooled fast reactor, J. Nucl. Sci. Technol. 48 (2011) 463–471.
[2] M. Ichimiya, T. Mizuno, S. Kotake, A next generation sodium-cooled fast reactor concept and its R&D program, Nucl. Eng. Technol. 39 (2007) 171–186.
[3] M. Konomura, M. Ichimiya, Design challenges for sodium cooled fast reactors, J. Nucl. Mater 371 (2007) 250–269.
[4] D. Hahn, J. Chang, Y.-I. Kim, Y.-I. Kim, Y.-I. Kim, C.B. Lee, S.-O. Kim, Advanced SFR design concepts and R&D activities, Nucl. Eng. Technol. 41 (2009) 427–446.
[5] J.-I. Saito, K. Ara, A study of atomic interaction between suspended nanoparticles and sodium atoms in liquid sodium, Nucl. Eng. Des. 240 (2010) 2664–2673.
[6] K. Ara, K. Sugiyama, H. Kitagawa, M. Nagai, N. Yoshioka, Study on chemical reactivity control of sodium by suspended nanoparticles I, J. Nucl. Sci. Technol. 47 (2010) 1165–1170.
[7] K. Ara, K. Sugiyama, H. Kitagawa, M. Nagai, N. Yoshioka, Study on chemical reactivity control of sodium by suspended nanoparticles II, J. Nucl. Sci. Technol. 47 (2010) 1171–1181.
[8] M. Nishimura, K. Nagai, T. Onojima, J.-I. Saito, K. Ara, K.-I. Sugiyama, The sodium oxidation reaction and suppression effect of sodium with suspended nanoparticles—growth behavior of dendritic oxide during oxidation, J. Nucl. Sci. Technol. 49 (2012) 71–77.
[9] J.-I. Saito, K. Ara, Chemical reactivity suppression of liquid sodium by suspended nanoparticles, Trans. Am. Nucl. Soc. 107 (2012) 433–436.
[10] J.-I. Saito, K. Nagai, K. Ara, Study on liquid sodium with suspended nanoparticles—(2) Atomic interaction and characteristics of liquid sodium with suspended nanoparticles, in: AIP Conference Proceedings, 2012.
[11] G. Park, S.J. Kim, M.H. Kim, H.S. Park, Experimental study of the role of nanoparticles in sodium–water reaction, Nucl. Eng. Des. 277 (2014) 46–54.
[12] S.J. Kim, G. Park, M.H. Kim, H.S. Park, J. Baek, A theoretical study of Ti nanoparticle effect on sodium water reaction: using *ab initio* calculation, Nucl. Eng. Des. 281 (2015) 15–21.
[13] J.N. Israelachvili, Intermolecular and Surface Forces, Revised Third Ed., Academic Press, USA, 2011.
[14] B. Derjaguin, Theory of the stability of strongly charged lyophobic sols and the adhesion of strongly charged particles in solutions of electrolytes, Acta Physicochim, USSR 14 (1941) 633–662.
[15] E.J.W. Verwey, J.T.G. Overbeek, K. Van Nes, Theory of the Stability of Lyophobic Colloids: the Interaction of Sol Particles Having an Electric Double Layer, Elsevier, New York, 1948.
[16] P. Debye, E. Hückel, De la théorie des électrolytes. i. abaissement du point de congélation et phénomènes associés, Phys. Z. 24 (1923) 185–206.
[17] D. Grasso, K. Subramaniam, M. Butkus, K. Strevett, J. Bergendahl, A review of non-DLVO interactions in environmental colloidal systems, Rev. Environ. Sci. Biotechnol. 1 (2002) 17–38.
[18] W. van Megen, I. Snook, Solvent structure and solvation forces between solid bodies, J. Chem. Soc. Faraday Trans. 2 Mol. Chem. Phys. 75 (1979) 1095–1102.

[19] W. Van Megen, I. Snook, Solvation forces in simple dense fluids. II. Effect of chemical potential, J. Chem. Phys. 74 (1981) 1409–1411.
[20] I. Snook, W. Van Megen, Solvation forces in simple dense fluids. III. Monolayer and submonolayer region, J. Chem. Phys. 75 (1981) 4738–4739.
[21] P. Attard, J.L. Parker, Oscillatory solvation forces: a comparison of theory and experiment, J. Phys. Chem. 96 (1992) 5086–5093.
[22] I. Snook, W. Van Megen, Solvation forces in simple dense fluids. I, J. Chem. Phys. 72 (2008) 2907–2913.
[23] H. Hamaker, The London–van der Waals attraction between spherical particles, Physica 4 (1937) 1058–1072.
[24] J.-N. Israelachvili, The calculation of van der Waals dispersion forces between macroscopic bodies, Proc. R. Soc. Lond, A Math. Phys. Sci. 331 (1972) 39–55.
[25] E. Lifshitz, The theory of molecular attractive forces between solids, Sov. Phys. JETP 2 (1956) 73–83.
[26] J.C. Sutherland, E. Araiawa, R. Hamm, Optical properties of sodium in the vacuum ultraviolet, J. Opt. Soc. Am. 57 (1967) 645–650.
[27] M.A. Ordal, L.L. Long, R.J. Bell, S.E. Bell, R.R. Bell, R.W. Alexander Jr., C.A. Ward, Optical properties of the metals Al, Co, Cu, Au, Fe, Pb, Ni, Pd, Pt, Ag, Ti, and W in the infrared and far infrared, Appl. Opt. 22 (1983) 1099–1119.
[28] B.V. Derjaguin, Untersuchungen über die Reibung und Adhäsion, IV, Coll. Polym. Sci. 69 (1934) 155–164.
[29] W.A. Steele, The physical interaction of gases with crystalline solids: I. Gas–solid energies and properties of isolated adsorbed atoms, Surf. Sci. 36 (1973) 317–352.
[30] J.E. Jones, On the determination of molecular fields. I. From the variation of the viscosity of a gas with temperature, in: Proceedings of the Royal Society of London. Series a, Containing Papers of a Mathematical and Physical Character, 1924, pp. 441–462.
[31] P. Hohenberg, W. Kohn, Inhomogeneous electron gas, Phys. Rev. 136 (1964) B864–B871.
[32] W. Kohn, L.J. Sham, Self-consistent equations including exchange and correlation effects, Phys. Rev. 140 (1965) A1133–A1138.
[33] P. Giannozzi, S. Baroni, N. Bonini, M. Calandra, R. Car, C. Cavazzoni, D. Ceresoli, G.L. Chiarotti, M. Cococcioni, I. Dabo, A. Dal Corso, S. de Gironcoli, S. Fabris, G. Fratesi, R. Gebauer, U. Gerstmann, C. Gougoussis, A. Kokalj, M. Lazzeri, L. Martin-Samos, N. Marzari, F. Mauri, R. Mazzarello, S. Paolini, A. Pasquarello, L. Paulatto, C. Sbraccia, S. Scandolo, G. Sclauzero, A.P. Seitsonen, A. Smogunov, P. Umari, R.M. Wentzcovitch, QUANTUM ESPRESSO: a modular and open-source software project for quantum simulations of materials, J. Phys. Condens. Matter 21 (2009) 395502 (19p).
[34] H.J. Monkhorst, J.D. Pack, Special points for Brillouin-zone integrations, Phys. Rev. B 13 (1976) 5188–5192.
[35] M. Methfessel, A. Paxton, High-precision sampling for Brillouin-zone integration in metals, Phys. Rev. B 40 (1989) 3616–3621.
[36] K.A. Fichthorn, Y. Qin, Molecular-dynamics simulation of colloidal nanoparticle forces, Ind. Eng. Chem. Res. 46 (2006) 5477–5481.
[37] K.A. Fichthorn, Y. Qin, Molecular dynamics simulation of the forces between colloidal nanoparticles in Lennard–Jones and n-decane solvent, Granular Matter 10 (2008) 105–111.
[38] Y. Qin, K.A. Fichthorn, Molecular-dynamics simulation of forces between nanoparticles in a Lennard–Jones liquid, J. Chem. Phys. 119 (2003) 9745–9754.
[39] M. Trautz, Das Gesetz der Reaktionsgeschwindigkeit und der Gleichgewichte in Gasen. Bestätigung der Additivität von Cv-3/2R. Neue Bestimmung der Integrationskonstanten und der Moleküldurchmesser, Z. Anorg, Allg. Chem. 96 (1916) 1–28.